

RESEARCH ARTICLE

Transferring entangled states of photonic cat-state qubits in circuit QED

Tong Liu¹, Zhen-Fei Zheng², Yu Zhang³, Yu-Liang Fang¹, Chui-Ping Yang^{1,†}¹Quantum Information Research Center, Shangrao Normal University, Shangrao 334001, China²Key Laboratory of Quantum Information, University of Science and Technology of China, Hefei 230026, China³School of Physics, Nanjing University, Nanjing 210093, ChinaCorresponding author. E-mail: †yangcp@hznju.edu.cn

Received September 30, 2019; accepted December 19, 2019

We propose a method for transferring quantum entangled states of two photonic cat-state qubits (*cqubits*) from two microwave cavities to the other two microwave cavities. This proposal is realized by using four microwave cavities coupled to a superconducting flux qutrit. Because of using four cavities with different frequencies, the inter-cavity crosstalk is significantly reduced. Since only one coupler qutrit is used, the circuit resource is minimized. The entanglement transfer is completed with a single-step operation only, thus this proposal is quite simple. The third energy level of the coupler qutrit is not populated during the state transfer, therefore decoherence from the higher energy level is greatly suppressed. Our numerical simulations show that high-fidelity transfer of two-*cqubit* entangled states from two transmission line resonators to the other two transmission line resonators is feasible with current circuit QED technology. This proposal is universal and can be applied to accomplish the same task in a wide range of physical systems, such as four microwave or optical cavities, which are coupled to a natural or artificial three-level atom.

Keywords transferring quantum entangled states, photonic cat-state, microwave cavities

1 Introduction

Circuit quantum electrodynamics (QED), consisting of superconducting (SC) qubits and microwave cavities or resonators, has developed fast in the past decade and has been considered as one of the most promising platforms for quantum information processing (QIP) [1–9]. SC qubits are good information carriers and units of quantum information processors due to controllability of their level spacings and recent significant improvement of their coherence times. It was theoretically predicted that the strong-coupling limit is readily achieved with SC charge qubits [3] or flux qubits [10], and later the strong and ultrastrong coupling between a SC qubit and a microwave resonator was experimentally demonstrated [11, 12] (hereafter, the terms cavity and resonator are used interchangeably). Based on circuit QED, many proposals have been presented for implementing quantum state transfer between SC qubits [1, 13–15], quantum logic gates of SC qubits [16–21], and entanglement in SC qubits [22–28]. By using SC qubits, the experimental demonstrations of single-qubit gates [29, 30], two-qubit gates [31, 32], three-qubit gates [33, 34], 10-qubit entanglement [35], 12-qubit entanglement [36], 18-qubit entanglement [37], and 20-qubit Schrödinger cat states [37] have been reported. Moreover, quantum teleportation between two distant SC qubits [38], quantum state transfer in a SC qubit chain [39], en-

tanglement swapping in superconducting circuit [40], and quantum walks in a 12-qubit superconducting processor [41] have been realized in experiments.

On the other hand, a (loaded) quality factor $Q = 10^6$ for a one-dimensional (1D) microwave resonator [42, 43] and a (loaded) quality factor $Q = 3.5 \times 10^7$ for a three-dimensional (3D) microwave resonator [44] have been reported experimentally. Photons, hosted by a microwave resonator or cavity with a high quality factor, have much longer lifetimes than SC qubits [45]. Hence, a microwave resonator or cavity of a high quality factor can behave as a quantum data bus and be used as quantum memory. In recent years, there is much interest in quantum state engineering and QIP with microwave fields or photons. Based on circuit QED, a number of proposals have been presented for creating Fock states [46], coherent states [47], squeezed states [48], macroscopic Schrödinger-cat states [49–52], and entangled states of microwave photons [53–61]. In addition, based on circuit QED, how to realize two-qubit or multi-qubit quantum gates with microwave photons has been investigated in theory [62–64]. The experimental preparations of a Fock state or a superposition of Fock states of photons [65–67], photonic Schrödinger cat states [68], and photonic NOON states [69] have been reported. The coherent transfer of single photons between microwave cavities has been demonstrated in experiments [70]. Moreover, quantum error correction and universal gate set on a binomial photonic logical qubit [71] have

been experimentally demonstrated.

The focus of this paper is on photonic cat-state qubits (*cqubits*). For a qubit, the two logic states are usually represented by two orthogonal cat states (i.e., superposition states of coherent states) of photons. In recent years, QIP with cqubits has attracted much attention because coherent states are eigenstates of the photon annihilation operator and tolerant to single-photon loss [72, 73] and the lifespan of a qubit can be greatly improved by quantum error correction [73]. Proposals for entangling qubits in a GHZ state [74] and for implementing single-qubit gates [75, 76], two-qubit gates [58, 77], and multi-target-qubit controlled gates [78] have been presented. Moreover, the experimental demonstration of single-qubit gates [79] and double-qubit entangled Bell states [80] has been reported. However, after in-depth search of literature, we found that how to directly transfer quantum entangled states of *cqubits* between cavities has not been studied yet.

In the following, we will propose a method to transfer quantum entangled states of two qubits from two microwave cavities to the other two microwave cavities via circuit QED. This proposal is realized by using a superconducting flux qutrit to couple four microwave cavities [Fig. 1(a)]. Throughout this paper, “qutrit” refers to a three-level quantum system. As shown below, this proposal has the following advantages: (i) Because of using four cavities with different frequencies, the inter-cavity crosstalk is greatly reduced; (ii) Due to the use of only one coupler qutrit, the circuit resources is minimized; (iii) The entanglement transfer is quite simple because only a single-step operation is needed; (iv) Because the higher energy level $|f\rangle$ of the coupler qutrit is not populated in the transfer process, the decoherence from this higher energy level is greatly inhibited; and (v) Neither measurement on the cavity state nor measurement on the qutrit state is required. In addition, our numerical simulations demonstrate that high-fidelity transfer of two-qubit entangled states from two transmission line resonators to the other two transmission line resonators is feasible with current circuit QED technology. This proposal is univer-

sal and can be applied to transfer two-qubit entangled states from two microwave or optical cavities to the other two cavities, which are coupled to a natural or artificial three-level atom.

This paper is organized as follows. In Section 2, we explicitly show how to transfer quantum entangled states of two qubits from two cavities to the other two cavities. In Section 3, we give a discussion on the experimental feasibility of the proposal. A concluding summary is presented in Section 4.

2 Transfer of quantum entangled states of two qubits

Consider four microwave cavities (1, 2, 3, 4) coupled to a superconducting flux qutrit [Fig. 1(a)]. The three levels of the coupler qutrit are labeled as $|g\rangle$, $|e\rangle$ and $|f\rangle$ [Fig. 1(b)]. Suppose that cavity 1 (3) is dispersively coupled to the $|g\rangle \leftrightarrow |f\rangle$ transition with coupling strength $g_1(g_3)$ and detuning $\Delta(\Delta')$, cavity 2 (4) is dispersively coupled to the $|e\rangle \leftrightarrow |f\rangle$ transition with coupling strength $g_2(g_4)$ and detuning $\Delta(\Delta')$, and each cavity is highly detuned (decoupled) from other energy level transitions [Fig. 1(b)]. Here, $\Delta = \omega_{fg} - \omega_1 = \omega_{fe} - \omega_2 > 0$ and $\Delta' = \omega_{fg} - \omega_3 = \omega_{fe} - \omega_4 < 0$, $\omega_{fg}(\omega_{fe})$ is the $|g\rangle \leftrightarrow |f\rangle$ ($|e\rangle \leftrightarrow |f\rangle$) transition frequency of the flux qutrit, and ω_j is the frequency of cavity j ($j = 1, 2, 3, 4$). In addition, apply a microwave pulse to the qutrit. The pulse is on resonance with the $|g\rangle \leftrightarrow |e\rangle$ transition but highly detuned (decoupled) from other energy level transitions [Fig. 1(b)]. These conditions can be met by prior adjustment of the qutrit’s level spacings or the cavity frequencies. Note that the level spacings of a superconducting qutrit can be rapidly (within 1–3 ns) adjusted [81] and the frequency of a microwave cavity can be fast tuned with a few nanoseconds [82].

Under the above considerations, the Hamiltonian of the whole system in the interaction picture and after the rotating wave approximation is given by (assuming $\hbar = 1$)

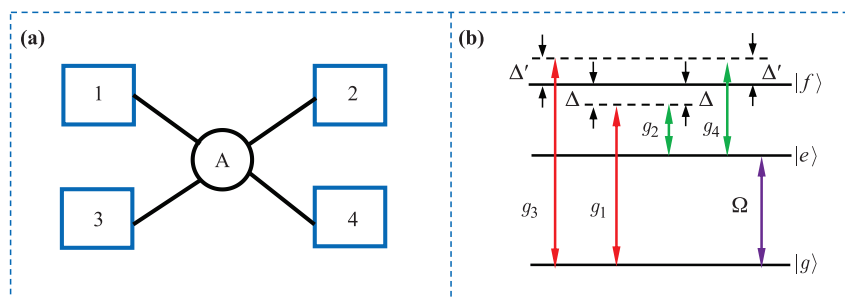


Fig. 1 (a) Diagram of a superconducting flux qutrit (a circle A at the center) and four microwave cavities. Each cavity here can be a three-dimensional (3D) cavity or a one-dimensional (1D) cavity. For 3D microwave cavities, the qutrit is inductively coupled to each cavity, by placing the qutrit’s partial loop area into each cavity. For 1D microwave cavities, the qutrit is capacitively coupled to each cavity (see Fig. 2). (b) Illustration of the qutrit-cavity dispersive interaction and the qutrit-pulse resonant interaction.

$$\begin{aligned}
 H = & \left(g_1 e^{i\Delta t} \hat{a}_1 \sigma_{fg}^+ + g_2 e^{i\Delta t} \hat{a}_2 \sigma_{fe}^+ \right) \\
 & + \left(g_3 e^{i\Delta' t} \hat{a}_3 \sigma_{fg}^+ + g_4 e^{i\Delta' t} \hat{a}_4 \sigma_{fe}^+ \right) + \Omega \sigma_{eg}^+ + \text{H.c.},
 \end{aligned}
 \tag{1}$$

where $\sigma_{fg}^+ = |f\rangle\langle g|$, $\sigma_{fe}^+ = |f\rangle\langle e|$, $\sigma_{eg}^+ = |e\rangle\langle g|$, Ω is the Rabi frequency of the pulse, and \hat{a}_j is the photon annihilation operator of cavity j ($j = 1, 2, 3, 4$).

In the large-detuning case of $\Delta \gg g_1, g_2$ and $|\Delta'| \gg g_3, g_4$, the intermediate level $|f\rangle$ can be adiabatically eliminated. As a result, the Raman couplings between the states $|g\rangle$ and $|e\rangle$ are induced by the cavity pairs (1, 2) and (3, 4). When $\frac{|\Delta - \Delta'|}{|\Delta - 1 + \Delta' - 1|} \gg g_1 g_4, g_2 g_3$, the Raman couplings between the states $|g\rangle$ and $|e\rangle$, caused by the cavity pairs (1, 4) and (2, 3), are suppressed because the corresponding effective coupling strengths are much smaller than the detunings of these Raman transitions. We assume $\Delta, |\Delta'| \gg \Omega$, for which the effect of the pulse on the Raman couplings is negligible. Thus, we can obtain the following effective Hamiltonian [83]

$$\begin{aligned}
 H_{\text{eff}} = & -2\lambda_1 \hat{a}_1^+ \hat{a}_1 \sigma_{gg} - 2\lambda_2 \hat{a}_2^+ \hat{a}_2 \sigma_{ee} \\
 & - 2\lambda_3 \hat{a}_3^+ \hat{a}_3 \sigma_{gg} - 2\lambda_4 \hat{a}_4^+ \hat{a}_4 \sigma_{ee} \\
 & - 2\lambda (\hat{a}_1 \hat{a}_2^+ \sigma_{eg}^+ + \hat{a}_1^+ \hat{a}_2 \sigma_{eg}^-) \\
 & - 2\lambda' (\hat{a}_3 \hat{a}_4^+ \sigma_{eg}^+ + \hat{a}_3^+ \hat{a}_4 \sigma_{eg}^-) \\
 & + \Omega \sigma_x,
 \end{aligned}
 \tag{2}$$

where $\sigma_{eg}^- = |g\rangle\langle e|$, $\sigma_{gg} = |g\rangle\langle g|$, $\sigma_{ee} = |e\rangle\langle e|$, $\sigma_x = \sigma_{eg}^+ + \sigma_{eg}^-$, $\lambda_1 = g_1^2/(2\Delta)$, $\lambda_2 = g_2^2/(2\Delta)$, $\lambda_3 = g_3^2/(2\Delta')$, $\lambda_4 = g_4^2/(2\Delta')$, $\lambda = g_1 g_2/(2\Delta)$, and $\lambda' = g_3 g_4/(2\Delta')$. Here, the terms in the first line are ac-Stark shifts of the level $|g\rangle$ ($|e\rangle$) induced by the cavity 1 (2), the terms in the second line are ac-Stark shifts of the level $|g\rangle$ ($|e\rangle$) induced by the cavity 3 (4), the terms in the third line represent the Raman coupling induced by the cavity pair (1, 2), while the terms in the fourth line represent the Raman coupling induced by the cavity pair (3, 4).

With definition of $|\pm\rangle = (|g\rangle \pm |e\rangle)/\sqrt{2}$, the operators of the coupler qutrit in Eq. (2) can be expressed as $\sigma_{gg} = (I + \tilde{\sigma}^+ + \tilde{\sigma}^-)/2$, $\sigma_{ee} = (I - \tilde{\sigma}^+ - \tilde{\sigma}^-)/2$, $\sigma_{eg}^+ = (\tilde{\sigma}_z + \tilde{\sigma}^+ - \tilde{\sigma}^-)/2$, $\sigma_{eg}^- = (\tilde{\sigma}_z - \tilde{\sigma}^+ + \tilde{\sigma}^-)/2$, and $\sigma_x = \tilde{\sigma}_z$, where $\tilde{\sigma}_z = |+\rangle\langle +| - |-\rangle\langle -|$, $\tilde{\sigma}^+ = |+\rangle\langle -|$, and $\tilde{\sigma}^- = |-\rangle\langle +|$. Using these expressions, one can rewrite Eq. (2), which will contain the terms $e^{-i2\Omega t}$ and $e^{i2\Omega t}$. In the strong driving regime $2\Omega \gg \lambda_1, \lambda_2, |\lambda_3|, |\lambda_4|, \lambda, |\lambda'|$, these terms oscillate with high frequencies and can be discarded after applying a rotating-wave approximation. Thus, it is easy to find that the Hamiltonian (2) becomes

$$\begin{aligned}
 \tilde{H}_{\text{eff}} = & -(\lambda_1 \hat{a}_1^+ \hat{a}_1 + \lambda_2 \hat{a}_2^+ \hat{a}_2 + \lambda_3 \hat{a}_3^+ \hat{a}_3 + \lambda_4 \hat{a}_4^+ \hat{a}_4) + \Omega \tilde{\sigma}_z \\
 & - \lambda (\hat{a}_1 \hat{a}_2^+ + \hat{a}_1^+ \hat{a}_2) \tilde{\sigma}_z - \lambda' (\hat{a}_3 \hat{a}_4^+ + \hat{a}_3^+ \hat{a}_4) \tilde{\sigma}_z.
 \end{aligned}
 \tag{3}$$

Performing a unitary transformation $e^{iH_0 t}$, with $H_0 = -(\lambda_1 \hat{a}_1^+ \hat{a}_1 + \lambda_2 \hat{a}_2^+ \hat{a}_2 + \lambda_3 \hat{a}_3^+ \hat{a}_3 + \lambda_4 \hat{a}_4^+ \hat{a}_4) + \Omega \tilde{\sigma}_z$, we obtain

$$\begin{aligned}
 H_e = & e^{iH_0 t} (\tilde{H}_{\text{eff}} - H_0) e^{-iH_0 t} \\
 = & -\lambda (\hat{a}_1 \hat{a}_2^+ + \hat{a}_1^+ \hat{a}_2) \tilde{\sigma}_z + \lambda (\hat{a}_3 \hat{a}_4^+ + \hat{a}_3^+ \hat{a}_4) \tilde{\sigma}_z,
 \end{aligned}
 \tag{4}$$

where we have set

$$\lambda_1 = \lambda_2, \quad \lambda_3 = \lambda_4,
 \tag{5}$$

$$\lambda = -\lambda'.
 \tag{6}$$

The qutrit is in the state $|+\rangle$, which can be easily prepared by applying a π -pulse resonant with the $|g\rangle \leftrightarrow |e\rangle$ transition of the qutrit initially in the ground state $|g\rangle$. Note that the qutrit remains in the state $|+\rangle$ because this state is not affected by the Hamiltonian (4). Hence, the qutrit part can be ignored and the effective Hamiltonian (4) further reduces to

$$H_e = H_{e1} + H_{e2},
 \tag{7}$$

with

$$H_{e1} = -\lambda (\hat{a}_1 \hat{a}_2^+ + \hat{a}_1^+ \hat{a}_2),
 \tag{8}$$

$$H_{e2} = \lambda (\hat{a}_3 \hat{a}_4^+ + \hat{a}_3^+ \hat{a}_4).
 \tag{9}$$

This Hamiltonian (7) describes the qutrit-mediated effective interaction between the cavity pair (1, 2) and the qutrit-mediated effective interaction between the cavity pair (3, 4), which will be used below to transfer quantum entangled states of two qubits from the two cavities (1, 2) to the other two cavities (3, 4).

Initially, cavities 1 and 3 store the maximally-entangled state $(|cat\rangle_1 |cat\rangle_3 + |\overline{cat}\rangle_1 |\overline{cat}\rangle_3)/\sqrt{2}$ of two qubits while cavities 2 and 4 are initially in the vacuum state $|0\rangle_2 |0\rangle_4$. Here, the two cat states are given by $|cat\rangle = N_\alpha^+ (|\alpha\rangle + |-\alpha\rangle)$ and $|\overline{cat}\rangle = N_\alpha^- (|\alpha\rangle - |-\alpha\rangle)$, with the normalization coefficients N_α^\pm . In terms of $|\alpha\rangle = e^{-|\alpha|^2/2} \sum_{n=0}^\infty \frac{\alpha^n}{\sqrt{n!}} |n\rangle$ and $|-\alpha\rangle = e^{-|\alpha|^2/2} \sum_{n=0}^\infty \frac{(-\alpha)^n}{\sqrt{n!}} |n\rangle$, we have

$$|cat\rangle = \sum_{m=0}^\infty C_{2m} |2m\rangle, \quad |\overline{cat}\rangle = \sum_{n=0}^\infty C_{2n+1} |2n+1\rangle,
 \tag{10}$$

where n and m are non-negative integers, $C_{2m} = 2N_\alpha^+ e^{-|\alpha|^2/2} \alpha^{2m} / \sqrt{(2m)!}$, and $C_{2n+1} = 2N_\alpha^- e^{-|\alpha|^2/2} \alpha^{2n+1} / \sqrt{(2n+1)!}$. From Eq. (10) one can see that the cat state $|cat\rangle$ is orthogonal to the cat state $|\overline{cat}\rangle$, independent of α (except for $\alpha = 0$). The two cat states considered here are called even and odd coherent states in quantum optics.

The transfer of the two-qubit entangled state from two cavities 1 and 3 to the other two cavities 2 and 4 is described by

$$\begin{aligned}
 & \frac{1}{\sqrt{2}} (|cat\rangle_1 |cat\rangle_3 + |\overline{cat}\rangle_1 |\overline{cat}\rangle_3) |0\rangle_2 |0\rangle_4 \\
 \rightarrow & |0\rangle_1 |0\rangle_3 \frac{1}{\sqrt{2}} (|cat\rangle_2 |cat\rangle_4 + |\overline{cat}\rangle_2 |\overline{cat}\rangle_4).
 \end{aligned}
 \tag{11}$$

In the following, we will show how this entangled state transfer can be achieved.

According to Eq. (10) and because of $|2m\rangle_j = (\hat{a}_j^\dagger)^{2m}|0\rangle_j/\sqrt{(2m)!}$ and $|2n+1\rangle_j = (\hat{a}_j^\dagger)^{2n+1}|0\rangle_j/\sqrt{(2n+1)!}$, the two cat states $|cat\rangle_j$ and $|\overline{cat}\rangle_j$ of cavity j ($j = 1, 2, 3, 4$) can be expressed as

$$\begin{aligned} |cat\rangle_j &= \sum_{m=0}^{\infty} C'_{2m} (\hat{a}_j^\dagger)^{2m} |0\rangle_j, \\ |\overline{cat}\rangle_j &= \sum_{n=0}^{\infty} C'_{2n+1} (\hat{a}_j^\dagger)^{2n+1} |0\rangle_j, \end{aligned} \quad (12)$$

where $C'_{2m} = C_{2m}/\sqrt{(2m)!}$ and $C'_{2n+1} = C_{2n+1}/\sqrt{(2n+1)!}$.

Under the effective Hamiltonian H_e of Eq. (7) and because of $[H_{e1}, H_{e2}] = 0$, we have the following state evolution

$$\begin{aligned} &e^{-iH_e t} |cat\rangle_1 |cat\rangle_3 |0\rangle_2 |0\rangle_4 \\ &= e^{-iH_{e1} t} |cat\rangle_1 |0\rangle_2 e^{-iH_{e2} t} |cat\rangle_3 |0\rangle_4 \\ &= \sum_{m=0}^{\infty} C'_{2m} e^{-iH_{e1} t} (\hat{a}_1^\dagger)^{2m} e^{iH_{e1} t} \otimes e^{-iH_{e1} t} |0\rangle_1 |0\rangle_2 \\ &\quad \otimes \sum_{m=0}^{\infty} C'_{2m} e^{-iH_{e2} t} (\hat{a}_3^\dagger)^{2m} e^{iH_{e2} t} \otimes e^{-iH_{e2} t} |0\rangle_3 |0\rangle_4 \\ &= \sum_{m=0}^{\infty} C'_{2m} (e^{-iH_{e1} t} \hat{a}_1^\dagger e^{iH_{e1} t})^{2m} |0\rangle_1 |0\rangle_2 \\ &\quad \otimes \sum_{m=0}^{\infty} C'_{2m} (e^{-iH_{e2} t} \hat{a}_3^\dagger e^{iH_{e2} t})^{2m} |0\rangle_3 |0\rangle_4, \end{aligned} \quad (13)$$

and

$$\begin{aligned} &e^{-iH_e t} |\overline{cat}\rangle_1 |\overline{cat}\rangle_2 |0\rangle_3 |0\rangle_4 \\ &= e^{-iH_{e1} t} |\overline{cat}\rangle_1 |0\rangle_2 e^{-iH_{e2} t} |\overline{cat}\rangle_2 |0\rangle_3 |0\rangle_4 \\ &= \sum_{n=0}^{\infty} C'_{2n+1} e^{-iH_{e1} t} (\hat{a}_1^\dagger)^{2n+1} e^{iH_{e1} t} \otimes e^{-iH_{e1} t} |0\rangle_1 |0\rangle_2 \\ &\quad \otimes \sum_{n=0}^{\infty} C'_{2n+1} e^{-iH_{e2} t} (\hat{a}_2^\dagger)^{2n+1} e^{iH_{e2} t} \otimes e^{-iH_{e2} t} |0\rangle_3 |0\rangle_4 \\ &= \sum_{n=0}^{\infty} C'_{2n+1} (e^{-iH_{e1} t} \hat{a}_1^\dagger e^{iH_{e1} t})^{2n+1} |0\rangle_1 |0\rangle_2 \end{aligned}$$

$$\otimes \sum_{n=0}^{\infty} C'_{2n+1} (e^{-iH_{e2} t} \hat{a}_3^\dagger e^{iH_{e2} t})^{2n+1} |0\rangle_3 |0\rangle_4, \quad (14)$$

where we have used $e^{-iH_{e1} t} |0\rangle_1 |0\rangle_2 = |0\rangle_1 |0\rangle_2$ and $e^{-iH_{e2} t} |0\rangle_3 |0\rangle_4 = |0\rangle_3 |0\rangle_4$.

Note that $e^{-iH_{e1} t} \hat{a}_1^\dagger e^{iH_{e1} t} = \cos(\lambda t) \hat{a}_1^\dagger + i \sin(\lambda t) \hat{a}_2^\dagger$ and $e^{-iH_{e2} t} \hat{a}_3^\dagger e^{iH_{e2} t} = \cos(\lambda t) \hat{a}_3^\dagger - i \sin(\lambda t) \hat{a}_4^\dagger$. For $\lambda t = \pi/2$, we have $e^{-iH_{e1} t} \hat{a}_1^\dagger e^{iH_{e1} t} = i \hat{a}_2^\dagger$ and $e^{-iH_{e2} t} \hat{a}_3^\dagger e^{iH_{e2} t} = -i \hat{a}_4^\dagger$. Thus, for $t = T = \pi/(2\lambda)$, we have from Eqs. (13) and (14)

$$\begin{aligned} &e^{-iH_e t} |cat\rangle_1 |cat\rangle_3 |0\rangle_2 |0\rangle_4 \\ &= |0\rangle_1 \sum_{m=0}^{\infty} C'_{2m} e^{im\pi} (\hat{a}_2^\dagger)^{2m} |0\rangle_2 \\ &\quad \otimes |0\rangle_3 \sum_{m=0}^{\infty} C'_{2m} e^{-im\pi} (\hat{a}_4^\dagger)^{2m} |0\rangle_4 \\ &= |0\rangle_1 \sum_{m=0}^{\infty} e^{im\pi} C'_{2m} |2m\rangle_2 \\ &\quad \otimes |0\rangle_3 \sum_{m=0}^{\infty} e^{-im\pi} C'_{2m} |2m\rangle_4, \end{aligned} \quad (15)$$

and

$$\begin{aligned} &e^{-iH_e t} |\overline{cat}\rangle_1 |\overline{cat}\rangle_2 |0\rangle_3 |0\rangle_4 \\ &= |0\rangle_1 \sum_{n=0}^{\infty} C'_{2n+1} e^{i(2n+1)\pi/2} (\hat{a}_2^\dagger)^{2n+1} |0\rangle_2 \\ &\quad \otimes |0\rangle_3 \sum_{n=0}^{\infty} C'_{2n+1} e^{-i(2n+1)\pi/2} (\hat{a}_4^\dagger)^{2n+1} |0\rangle_4 \\ &= |0\rangle_1 \sum_{n=0}^{\infty} e^{i(2n+1)\pi/2} C'_{2n+1} |2n+1\rangle_2 \\ &\quad \otimes |0\rangle_3 \sum_{n=0}^{\infty} e^{-i(2n+1)\pi/2} C'_{2n+1} |2n+1\rangle_4, \end{aligned} \quad (16)$$

where we have used $|2m\rangle_j = (\hat{a}_j^\dagger)^{2m}|0\rangle_j/\sqrt{(2m)!}$, $|2n+1\rangle_j = (\hat{a}_j^\dagger)^{2n+1}|0\rangle_j/\sqrt{(2n+1)!}$ ($j = 2, 4$), and the definitions of C'_{2m} and C'_{2n+1} given above.

After returning to the original interaction picture, the time evolution for the initial state of the whole system is given by

$$\begin{aligned} &e^{-iH_0 \tau} e^{-iH_e \tau} \frac{1}{\sqrt{2}} (|cat\rangle_1 |cat\rangle_3 + |\overline{cat}\rangle_1 |\overline{cat}\rangle_3) |0\rangle_2 |0\rangle_4 |+\rangle \\ &= e^{-iH_0 \tau} \frac{1}{\sqrt{2}} \left(|0\rangle_1 \sum_{m=0}^{\infty} e^{im\pi} C'_{2m} |2m\rangle_2 \otimes |0\rangle_3 \sum_{m=0}^{\infty} e^{-im\pi} C'_{2m} |2m\rangle_4 \right. \\ &\quad \left. + |0\rangle_1 \sum_{n=0}^{\infty} e^{i(2n+1)\pi/2} C'_{2n+1} |2n+1\rangle_2 \otimes |0\rangle_3 \sum_{n=0}^{\infty} e^{-i(2n+1)\pi/2} C'_{2n+1} |2n+1\rangle_4 \right) |+\rangle \end{aligned}$$

$$\begin{aligned}
 &= e^{-i\phi_0} |0\rangle_1 |0\rangle_3 \frac{1}{\sqrt{2}} \left[\sum_{m=0}^{\infty} e^{i2\eta m\pi} C_{2m} |2m\rangle_2 \otimes \sum_{m=0}^{\infty} e^{i2\eta' m\pi} C_{2m} |2m\rangle_4 \right. \\
 &\quad \left. + \sum_{n=0}^{\infty} e^{i\eta(2n+1)\pi} C_{2n+1} |2n+1\rangle_2 \otimes \sum_{n=0}^{\infty} e^{i\eta'(2n+1)\pi} C_{2n+1} |2n+1\rangle_4 \right] |+\rangle, \tag{17}
 \end{aligned}$$

where from line 1 to lines 2 and 3 we have used the results given in Eqs. (15) and (16). Here, $\phi_0 = \Omega\pi/(2\lambda)$, $\eta = \lambda_2/(2\lambda) + 1/2$, and $\eta' = \lambda_4/(2\lambda) - 1/2$. We set

$$\lambda_2 = \lambda, \tag{18}$$

$$\lambda_4 = -\lambda, \tag{19}$$

which leads to $\eta = 1$ and $\eta' = -1$. For $\eta = 1$ and $\eta' = -1$, we have $\exp(i2\eta m\pi) = \exp(i2\eta' m\pi) = 1$ and $\exp[i\eta(2n+1)\pi] = \exp[i\eta'(2n+1)\pi] = -1$. Thus, the state of the four cavities, given in Eq. (17), becomes

$$\begin{aligned}
 &|0\rangle_1 |0\rangle_3 \frac{1}{\sqrt{2}} \left(\sum_{m=0}^{\infty} C_{2m} |2m\rangle_2 \otimes \sum_{m=0}^{\infty} C_{2m} |2m\rangle_4 \right. \\
 &\quad \left. + \sum_{n=0}^{\infty} C_{2n+1} |2n+1\rangle_2 \otimes \sum_{n=0}^{\infty} C_{2n+1} |2n+1\rangle_4 \right), \tag{20}
 \end{aligned}$$

where the common phase factor $e^{-i\phi_0}$ has been omitted. According to Eq. (12), the state (20) can be written as

$$|0\rangle_1 |0\rangle_3 \frac{1}{\sqrt{2}} (|cat\rangle_2 |cat\rangle_4 + |\overline{cat}\rangle_2 |\overline{cat}\rangle_4), \tag{21}$$

which shows that the quantum entangled state of two qubits, originally stored in the two cavities 1 and 3, has been transferred onto the other two cavities 2 and 4. In order to maintain the transferred state, the level spacings of the flux qutrit need to be rapidly adjusted [81] so that the qutrit is decoupled from four cavities after the desired state transfer is completed. Alternatively, to have the cavities coupled or decoupled from the qutrit, one can also tune the frequencies of cavities [82].

The result (21) was derived under the conditions (5), (6), (18) and (19) given above. The conditions (5) and (6) can be satisfied by choosing $g_1 = g_2$ and $g_3 = g_4$. This requirement for the coupling constants can be achieved for either 3D cavities or 1D cavities. For 3D cavities, g_j can be adjusted by a prior design of the sample with a suitable loop area of the qutrit that falls in cavity j ($j = 1, 2, 3, 4$). In addition, for 1D cavities, g_j can be adjusted by a prior design of the sample with an appropriate capacitance C_j between the qutrit and cavity j ($j = 1, 2, 3, 4$).

One can check that both conditions (6) and (19) turn out into

$$g_1 g_2 / \Delta = -g_3 g_4 / \Delta', \tag{22}$$

i.e.,

$$\begin{aligned}
 g_1 g_2 / (\omega_{fg} - \omega_1) &= g_1 g_2 / (\omega_{fe} - \omega_2) \\
 &= g_3 g_4 / (\omega_3 - \omega_{fg}) \\
 &= g_3 g_4 / (\omega_4 - \omega_{fe}), \tag{23}
 \end{aligned}$$

which can be met by adjusting the cavity frequencies, the qutrit level spacings, or the coupling constants.

From the above description, one can see that the coupler qutrit remains in the state $|+\rangle$ during the state transfer. In other words, the level $|f\rangle$ of the qutrit is not excited and thus decoherence from this higher energy level is greatly suppressed. Eq. (17) shows that the state transfer is performed by applying a unitary operator $U = e^{-iH_0\tau} e^{-iH_e\tau}$ on the initial state of the whole system. As mentioned above, the transformation $e^{-iH_0\tau}$ here is only used in order to return to the original interaction picture. Thus, it can be concluded that the state transfer is realized with a single-step operation, described by U .

3 Possible experimental implementation

In above, we have considered a general type of cavity, either 3D cavity or 1D cavity. In this section, we consider a setup of four transmission line resonators (TLRs) capacitively coupled to a superconducting flux qutrit (Fig. 2). Each TLR here is a 1D microwave cavity. For a flux device (e.g., C-shunted flux qubit [84–86]), the level spacings can be designed to have a sufficiently large anharmonicity and the transition between non-adjacent levels is allowed. Accordingly, our proposal uses the flux qutrit so that the resonator coupling with the flux qutrit's $|g\rangle \leftrightarrow |f\rangle$ transition is available. In the following, we will give a discussion on the experimental feasibility of transferring quantum entangled states of two qubits between the two TLRs.

By taking the unwanted interaction into account, the

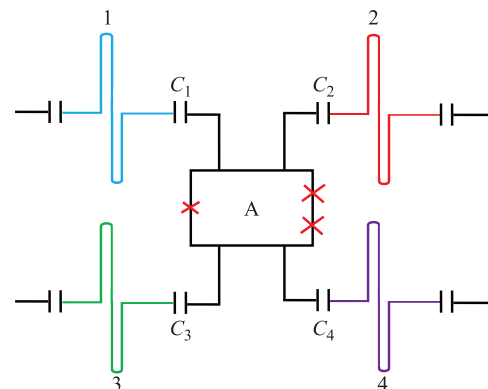


Fig. 2 Setup of four transmission line resonators (TLRs) capacitively coupled to a superconducting flux qutrit (a square A at the center). The flux qutrit consists of three Josephson junctions and a superconducting loop.

Hamiltonian (1) is modified as $H' = H + \delta H_1 + \delta H_2$. Here, δH_1 describes the unwanted inter-cavity crosstalk, with the form of

$$\delta H_1 = \sum_{j=1}^4 \sum_{l=j+1}^4 g_{jl} e^{i\Delta_{jl}t} \hat{a}_j \hat{a}_l^\dagger + \text{H.c.}, \quad (24)$$

where g_{jl} and $\Delta_{jl} = \omega_l - \omega_j$ are, respectively, the coupling strength and the frequency detuning of the two cavities j and l ($jl = 12, 13, 14, 23, 24, 34$). In addition, δH_2 describes the unwanted $|e\rangle \leftrightarrow |f\rangle$ transition induced by the pulse, which is given by

$$\delta H_2 = \Omega_{fe} e^{i\Delta_p t} S_{fe}^+ + \text{H.c.}, \quad (25)$$

where $\Delta_p = \omega_{fe} - \omega_{eg}$, and Ω_{fe} is the Rabi frequency of the pulse, associated with the $|e\rangle \leftrightarrow |f\rangle$ transition.

Because of $\omega_{eg} \ll \omega_{fg}$ [Fig. 1(b)], the $|g\rangle \leftrightarrow |f\rangle$ transition induced by the pulse is negligible. For a superconducting flux device, the level spacings can be designed to have a sufficiently large anharmonicity, such that the cavity-induced coherent transitions between any other irrelevant levels are negligibly small. Hence, the effects of the cavity-induced unwanted transitions as well as the pulse-induced $|g\rangle \leftrightarrow |f\rangle$ transition on the state transfer performance are negligible and thus not considered in our numerical simulations for simplicity.

After considering the qutrit dephasing and energy relaxation and the cavity dissipation, the system dynamics under Markovian approximation is governed by the master equation

$$\begin{aligned} \frac{d\rho}{dt} = & -i[H', \rho] + \sum_{j=1}^4 \kappa_j \mathcal{L}[\hat{a}_j] \\ & + \gamma_{fe} \mathcal{L}[\sigma_{fe}^-] + \gamma_{fg} \mathcal{L}[\sigma_{fg}^-] + \gamma_{eg} \mathcal{L}[\sigma_{eg}^-] \\ & + \sum_{l=e,f} \gamma_{\varphi,l} (\sigma_{ll} \rho \sigma_{ll} - \sigma_{ll} \rho / 2 - \rho \sigma_{ll} / 2). \end{aligned} \quad (26)$$

Here, $\mathcal{L}[\Lambda] = \Lambda \rho \Lambda^\dagger - \Lambda^\dagger \Lambda \rho / 2 - \rho \Lambda^\dagger \Lambda / 2$ (with $\Lambda = \hat{a}_j, \sigma_{fe}^-, \sigma_{fg}^-, \sigma_{eg}^-$), and $\sigma_{ff} = |f\rangle\langle f|$; κ_j is the decay rate of cavity j ($j = 1, 2, 3, 4$); γ_{eg} is the energy relaxation rate for the level $|e\rangle$ of the qutrit, associated with the decay path $|e\rangle \rightarrow |g\rangle$; γ_{fe} (γ_{fg}) is the relaxation rate for the level $|f\rangle$ of the qutrit, related to the decay path $|f\rangle \rightarrow |e\rangle$ ($|f\rangle \rightarrow |g\rangle$); $\gamma_{\varphi,e}$ ($\gamma_{\varphi,f}$) is the dephasing rate of the level $|e\rangle$ ($|f\rangle$).

The fidelity of the entangled state transfer is given by $\mathcal{F} = \sqrt{\langle \psi_{\text{id}} | \tilde{\rho} | \psi_{\text{id}} \rangle}$, where $|\psi_{\text{id}}\rangle$ is the ideal output state of the four cavities given in Eq. (21), while $\tilde{\rho}$ is the reduced density operator of the four cavities after tracing ρ over the degrees of the coupler qutrit, when the state transfer is carried out in a realistic system (with dissipation and dephasing considered). Note that our numerical simulations are performed by choosing the operation time $t = \pi / (2\lambda)$ above.

For a three-level flux qutrit, the transition frequency between two neighboring levels can be varied from 5 GHz

to 20 GHz. As an example, we consider $\omega_{eg}/2\pi = 7.5$ GHz and $\omega_{fg}/2\pi = 12.5$ GHz, resulting in $\Delta_p/2\pi = -2.5$ GHz. We choose $\Delta/2\pi = 800$ MHz, $g_1/2\pi = g_2/2\pi = 60$ MHz, and $g_3/2\pi = g_4/2\pi = 70$ MHz. According to Eq. (22), a simple calculation gives $\Delta'/2\pi \sim -1.09$ GHz. Note that the coupling constants here are readily achievable in experiments because a coupling strength ~ 636 MHz was reported for a superconducting flux device coupled to a TLR [12]. The detunings here yields $\omega_1/2\pi = 11.7$ GHz, $\omega_2/2\pi = 4.2$ GHz, $\omega_3/2\pi = 13.59$ GHz, $\omega_4/2\pi = 6.09$ GHz. Thus, we have $\Delta_{12}/2\pi = -7.5$ GHz, $\Delta_{13}/2\pi = 1.89$ GHz, $\Delta_{14}/2\pi = -5.61$ GHz, $\Delta_{23}/2\pi = 9.39$ GHz, $\Delta_{24}/2\pi = 1.89$ GHz, and $\Delta_{34}/2\pi = -7.5$ GHz. For simplicity, we choose $\Omega_{fe}/2\pi = \Omega/2\pi = 47$ MHz (available in experiments [87, 88]). Other parameters used in the numerical simulation are: (i) $\gamma_{\varphi,e}^{-1} = \gamma_{\varphi,f}^{-1} = 7$ μs , $\gamma_{fe}^{-1} = 28$ μs , $\gamma_{fg}^{-1} = 14$ μs , $\gamma_{fg}^{-1} = 21$ μs (a conservative consideration, e.g., see Refs. [84–86]); (ii) $\kappa_1^{-1} = \kappa_2^{-1} = \kappa_3^{-1} = \kappa_4^{-1} = \kappa^{-1}$; and (iii) $\alpha = 1.5$.

We now numerically calculate the fidelity for the entangled state transfer. For simplicity, we assume that the crosstalk strength for every two cavities is equal, and thus we set $g_{jl} \equiv g_{cr}$ ($jl = 12, 13, 14, 23, 24, 34$). To see how the inter-cavity crosstalk and the cavity decay affect the operation performance, we plot Fig. 3 to show the fidelity \mathcal{F} versus κ^{-1} and g_{cr}/g_m . Here, $g_m = \max\{g_1, g_2, g_3, g_4\}$. From Fig. 3, one can see that the effect of the inter-cavity crosstalk coupling is very small for a given κ^{-1} . One can see that even when $g_{cr} = 0.1g_m$, a high fidelity $\sim 98.7\%$ can be reached for $\kappa^{-1} = 10$ μs . Note that the crosstalk strength between cavities can be made $0.01g_m$ by a prior design of the sample with appropriate capacitances C_1, C_2, C_3, C_4 [54].

To investigate the effect of the decay of the second excited state (i.e., $|f\rangle$) of the qutrit on the fidelity, we numerically calculate the operation fidelity for the entangled state transfer for (i) $\gamma_{\varphi,f}^{-1} = 7$ μs , $\gamma_{fe}^{-1} = 14$ μs , $\gamma_{fg}^{-1} = 21$ μs and (ii) $\gamma_{\varphi,f}^{-1} = \gamma_{fe}^{-1} = \gamma_{fg}^{-1} = 0$ μs , as the blue and red lines displayed in Fig. 4. Figure 4 shows the fidelity \mathcal{F} versus κ^{-1} , which is plotted for $g_{cr} = 0.01g_m$. Other parameters used in the numerical simulation for Fig. 4 are the same as those used in Fig. 3. From Fig. 4, one can

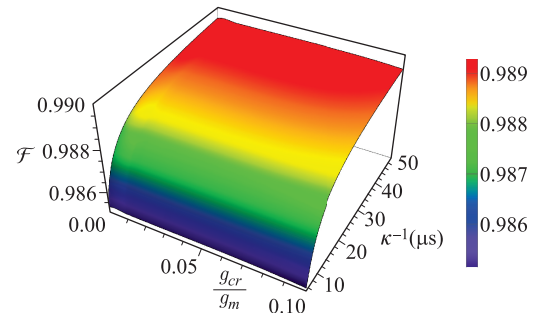


Fig. 3 Fidelity \mathcal{F} versus κ^{-1} and g_{cr}/g_m . The parameters used in the numerical simulation are referred to the text.

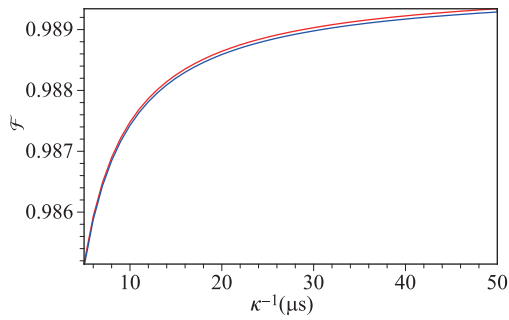


Fig. 4 Fidelity \mathcal{F} versus κ^{-1} . The red line correspond to the case without considering the decay of the second excited state of the qutrit, while the blue line correspond to the case that the decay of the second excited state of the qutrit is taken into account.

see that for $\kappa^{-1} = 10 \mu\text{s}$, a high fidelity $\sim 98.747\%$ or $\sim 98.748\%$ is achievable for (i) or (ii). Figure 4 displays the effect of the decay of the second excited state of the qutrit is negligible.

In addition, we also give the numerical results of the population of the second excited state of the qutrit in Fig. 5. Figure 5 displays the population P_f of the second excited state of the qutrit versus t/T for the entangled state transfer, which is plotted for $g_{cr} = 0.01g_m$. Here, t is the state evolution time and T is the entire operation time required for the state transfer. Other parameters chosen are the same as those used in Fig. 3. Figure 5 shows that the population of the second excited state of the qutrit is less than 0.014, implying that the second excited state of the qutrit is almost not populated during the entire operation. Thus, the decoherence of the qutrit from the second excited state can be efficiently suppressed.

In practice, it is an experimental challenge to have $g_1 = g_2$ and $g_3 = g_4$. Thus, for the sake of generality, we consider $g_2 = (1 + \epsilon)g_1$ and $g_4 = (1 + \epsilon)g_3$, with the values of g_1 and g_2 given above. We plot Fig. 6 to show how the fidelity \mathcal{F} changes with ϵ . Figure 6 is plotted for $\kappa^{-1} = 10 \mu\text{s}$ and $g_{cr} = 0, 0.01g_m, 0.1g_m$. Other parameters chosen are the same as those given in Fig. 3. From

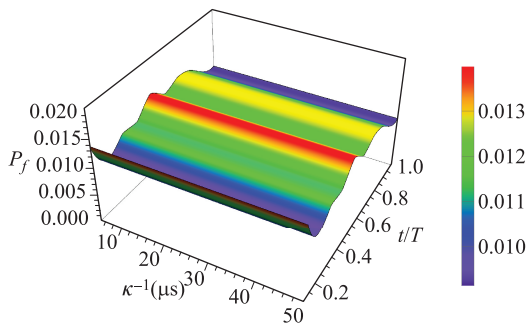


Fig. 5 The population P_f of the second excited state of the qutrit versus t/T , which is plotted for $g_{cr} = 0.01g_m$. Other parameters chosen are the same as those used in Fig. 3.

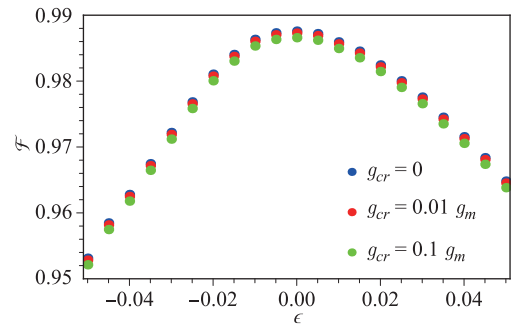


Fig. 6 Fidelity \mathcal{F} versus ϵ . The figure is plotted for $g_{cr} = 0, 0.01g_m, 0.1g_m$ and $\kappa^{-1} = 10 \mu\text{s}$. Other parameters used in the numerical simulation are the same as those used in Fig. 3.

Fig. 6, one can see that the fidelity strongly depends on ϵ , but a high fidelity $\gtrsim 95.3\%$ can still be available for $-5\% \leq \epsilon \leq 5\%$.

With the parameters chosen above, the operational time is estimated as $0.11 \mu\text{s}$, much shorter than the decoherence times of the qutrit used in the numerical simulation and the cavity decay times ($5\text{--}50 \mu\text{s}$) considered in Fig. 3. For the cavity frequencies given above and for $\kappa^{-1} = 10 \mu\text{s}$ used in the numerical simulation, the required quality factors ($Q_j = \kappa_j^{-1}\omega_j$) for the four cavities are $Q_1 \sim 7.35 \times 10^5$, $Q_2 \sim 2.64 \times 10^5$, $Q_3 \sim 8.53 \times 10^5$, $Q_4 \sim 3.82 \times 10^5$. The cavity quality factors here are achievable in experiment because TLRs with a (loaded) quality factor $Q \sim 10^6$ have been experimentally demonstrated [42, 43]. The analysis here demonstrates that the high-fidelity transfer of quantum entangled states of two cat-state qubits, from two microwave cavities to the other two microwave cavities, is feasible within present-day circuit QED techniques.

4 Conclusion

We have presented an approach to transfer quantum entangled states of two cat-state qubits based on circuit QED. As shown above, this proposal has the advantages stated in the introduction. Our numerical simulations demonstrate that high-fidelity transfer of quantum entangled states of two cat-state qubits from two TLRs to the other two TLRs is feasible with current circuit QED technology. This proposal is quite general and can be applied to transfer quantum entangled states of two cat-state qubits in a wide range of physical systems, such as four 1D or 3D (microwave or optical) cavities coupled to a natural or artificial three-level atom. To the best of our knowledge, this work is the first to demonstrate the transfer of quantum entangled states of cat-state qubits, based on circuit or cavity QED. We hope that this work will stimulate the experimental activity in the near future.

Acknowledgements This work was partly supported by the Key-Area Research and Development Program of Guangdong

Province (Grant No. 2018B030326001), the National Natural Science Foundation of China (NSFC) (Grant Nos. 11074062, 11374083, and 11774076), the NKRD of China (Grant No. 2016YFA0301802), and the Jiangxi Natural Science Foundation (Grant No. 20192ACBL20051).

References

1. C. P. Yang, S. I. Chu, and S. Han, Possible realization of entanglement, logical gates, and quantum information transfer with superconducting-quantuminterference-device qubits in cavity QED, *Phys. Rev. A* 67(4), 042311 (2003)
2. J. Q. You and F. Nori, Quantum information processing with superconducting qubits in a microwave field, *Phys. Rev. B* 68(6), 064509 (2003)
3. A. Blais, R. S. Huang, A. Wallraff, S. M. Girvin, and R. J. Schoelkopf, Cavity quantum electrodynamics for superconducting electrical circuits: An architecture for quantum computation, *Phys. Rev. A* 69(6), 062320 (2004)
4. J. Q. You and F. Nori, Superconducting circuits and quantum information, *Phys. Today* 58(11), 42 (2005)
5. J. Clarke and F. K. Wilhelm, Superconducting quantum bits, *Nature* 453(7198), 1031 (2008)
6. J. Q. You and F. Nori, Atomic physics and quantum optics using superconducting circuits, *Nature* 474(7353), 589 (2011)
7. Z. L. Xiang, S. Ashhab, J. Q. You, and F. Nori, Hybrid quantum circuits: Superconducting circuits interacting with other quantum systems, *Rev. Mod. Phys.* 85(2), 623 (2013)
8. X. Gu, A. F. Kockum, A. Miranowicz, Y. X. Liu, and F. Nori, Microwave photonics with superconducting quantum circuits, *Phys. Rep.* 718–719, 1 (2017)
9. P. B. Li, Y. C. Liu, S. Y. Gao, Z. L. Xiang, P. Rabl, Y. F. Xiao, and F. L. Li, Hybrid quantum device based on NV centers in diamond nanomechanical resonators plus superconducting waveguide cavities, *Phys. Rev. Appl.* 4(4), 044003 (2015)
10. C. P. Yang, S. I. Chu, and S. Han, Quantum information transfer and entanglement with SQUID qubits in cavity QED: A dark-state scheme with tolerance for nonuniform device parameter, *Phys. Rev. Lett.* 92(11), 117902 (2004)
11. A. Wallraff, D. I. Schuster, A. Blais, L. Frunzio, R. S. Huang, J. Majer, S. Kumar, S. M. Girvin, and R. J. Schoelkopf, Strong coupling of a single photon to a superconducting qubit using circuit quantum electrodynamics, *Nature* 431(7005), 162 (2004)
12. T. Niemczyk, F. Deppe, H. Huebl, E. P. Menzel, F. Hocke, M. J. Schwarz, J. J. Garcia-Ripoll, D. Zueco, T. Hümmer, E. Solano, A. Marx, and R. Gross, Circuit quantum electrodynamics in the ultrastrong coupling regime, *Nat. Phys.* 6(10), 772 (2010)
13. Q. Q. Wu, J. Q. Liao, and L. M. Kuang, Quantum state transfer between charge and flux qubits in circuit-QED, *Chin. Phys. Lett.* 25(4), 1179 (2008)
14. Z. B. Feng, Quantum state transfer between hybrid qubits in a circuit QED, *Phys. Rev. A* 85(1), 014302 (2012)
15. C. P. Yang, Q. P. Su, and F. Nori, Entanglement generation and quantum information transfer between spatially-separated qubits in different cavities, *New J. Phys.* 15(11), 115003 (2013)
16. C. P. Yang and S. Han, n -qubit-controlled phase gate with superconducting quantum interference devices coupled to a resonator, *Phys. Rev. A* 72(3), 032311 (2005)
17. C. P. Yang, Y. X. Liu, and F. Nori, Phase gate of one qubit simultaneously controlling n qubits in a cavity, *Phys. Rev. A* 81(6), 062323 (2010)
18. C. P. Yang, Q. P. Su, F. Y. Zhang, and S. B. Zheng, Single-step implementation of a multiple target-qubit controlled phase gate without need of classical pulses, *Opt. Lett.* 39(11), 3312 (2014)
19. H. F. Wang, A. D. Zhu, and S. Zhang, One-step implementation of a multiqubit phase gate with one control qubit and multiple target qubits in coupled cavities, *Opt. Lett.* 39(6), 1489 (2014)
20. Z. P. Hong, B. J. Liu, J. Q. Cai, X. D. Zhang, Y. Hu, Z. D. Wang, and Z. Y. Xue, Implementing universal nonadiabatic holonomic quantum gates with transmons, *Phys. Rev. A* 97(2), 022332 (2018)
21. B. Ye, Z. F. Zheng, and C. P. Yang, Multiplex-controlled phase gate with qubits distributed in a multicavity system, *Phys. Rev. A* 97(6), 062336 (2018)
22. S. L. Zhu, Z. D. Wang, and P. Zanardi, Geometric quantum computation and multiqubit entanglement with superconducting qubits inside a cavity, *Phys. Rev. Lett.* 94(10), 100502 (2005)
23. X. L. Zhang, K. L. Gao, and M. Feng, Preparation of cluster states and W states with superconducting quantum-interference-device qubits in cavity QED, *Phys. Rev. A* 74(2), 024303 (2006)
24. Z. J. Deng, K. L. Gao, and M. Feng, Generation of N-qubit W states with rf SQUID qubits by adiabatic passage, *Phys. Rev. A* 74(6), 064303 (2006)
25. F. Helmer, and F. Marquardt, Measurement-based synthesis of multiqubit entangled states in superconducting cavity QED, *Phys. Rev. A* 79(5), 052328 (2009)
26. S. Aldana, Y. D. Wang, and C. Bruder, Greenberger-Horne-Zeilinger generation protocol for N superconducting transmon qubits capacitively coupled to a quantum bus, *Phys. Rev. B* 84(13), 134519 (2011)
27. C. P. Yang, Q. P. Su, S. B. Zheng, and F. Nori, Entangling superconducting qubits in a multi-cavity system, *New J. Phys.* 18(1), 013025 (2016)
28. X. T. Mo, and Z. Y. Xue, Single-step multipartite entangled states generation from coupled circuit cavities, *Front. Phys.* 14(3), 31602 (2019)
29. Y. Xu, W. Cai, Y. Ma, X. Mu, L. Hu, T. Chen, H. Wang, Y. P. Song, Z. Y. Xue, Z. Q. Yin, and L. Sun, Single-loop realization of arbitrary non-adiabatic holonomic single-qubit quantum gates in a superconducting circuit, *Phys. Rev. Lett.* 121(11), 110501 (2018)

30. T. Wang, Z. Zhang, L. Xiang, Z. Jia, P. Duan, W. Cai, Z. Gong, Z. Zong, M. Wu, J. Wu, L. Sun, Y. Yin, and G. Guo, The experimental realization of high-fidelity “shortcut-to-adiabaticity” quantum gates in a superconducting Xmon qubit, arXiv: 1804.08247 (2018)
31. P. J. Leek, S. Filipp, P. Maurer, M. Baur, R. Bianchetti, J. M. Fink, M. Göppl, L. Steffen, and A. Wallraff, Using sideband transitions for two-qubit operations in superconducting circuits, *Phys. Rev. B* 79, 180511(R) (2009)
32. J. M. Chow, A. D. Córcoles, J. M. Gambetta, C. Rigetti, B. R. Johnson, J. A. Smolin, J. R. Rozen, G. A. Keefe, M. B. Rothwell, M. B. Ketchen, and M. Steffen, Simple All-microwave entangling gate for fixed-frequency superconducting qubits, *Phys. Rev. Lett.* 107(8), 080502 (2011)
33. M. Mariantoni, H. Wang, T. Yamamoto, M. Neeley, R. C. Bialczak, Y. Chen, M. Lenander, E. Lucero, A. D. O’Connell, D. Sank, M. Weides, J. Wenner, Y. Yin, J. Zhao, A. N. Korotkov, A. N. Cleland, and J. M. Martinis, Implementing the quantum von neumann architecture with superconducting circuits, *Science* 334(6052), 61 (2011)
34. A. Fedorov, L. Steffen, M. Baur, M. P. daSilva, and A. Wallraff, Implementation of a Toffoli gate with superconducting circuits, *Nature* 481(7380), 170 (2012)
35. C. Song, K. Xu, W. Liu, C. Yang, S. B. Zheng, H. Deng, Q. Xie, K. Huang, Q. Guo, L. Zhang, P. Zhang, D. Xu, D. Zheng, X. Zhu, H. Wang, Y.A. Chen, C.Y. Lu, S. Han, and J.W. Pan, 10-qubit entanglement and parallel logic operations with a superconducting circuit, *Phys. Rev. Lett.* 119(18), 180511 (2017)
36. M. Gong, M. C. Chen, Y. Zheng, S. Wang, C. Zha, H. Deng, Z. Yan, H. Rong, Y. Wu, S. Li, F. Chen, Y. Zhao, F. Liang, J. Lin, Y. Xu, C. Guo, L. Sun, A. D. Castellano, H. Wang, C. Peng, C.Y. Lu, X. Zhu, and J.W. Pan, Genuine12-qubit entanglement on a superconducting quantum processor, *Phys. Rev. Lett.* 122(11), 110501 (2019)
37. C. Song, K. Xu, H. Li, Y. Zhang, X. Zhang, W. Liu, Q. Guo, Z. Wang, W. Ren, J. Hao, H. Feng, H. Fan, D. Zheng, D. Wang, H. Wang, and S. Zhu, Observation of multi-component atomic Schrödinger cat states of up to 20 qubits, *Science* 365(6453), 574 (2019)
38. L. Steffen, Y. Salathe, M. Oppliger, P. Kurpiers, M. Baur, C. Lang, C. Eichler, G. Puebla-Hellmann, A. Fedorov, and A. Wallraff, Deterministic quantum teleportation with feed-forward in a solid state system., *Nature* 500(7462), 319 (2013)
39. X. Li, Y. Ma, J. Han, T. Chen, Y. Xu, W. Cai, H. Wang, Y. P. Song, Z. Y. Xue, Z. Q. Yin, and L. Sun, Perfect quantum state transfer in a superconducting qubit chain with parametrically tunable couplings, *Phys. Rev. Appl.* 10(5), 054009 (2018)
40. W. Ning, X. J. Huang, P. R. Han, H. Li, H. Deng, Z. B. Yang, Z. R. Zhong, Y. Xia, K. Xu, D. Zheng, and S. B. Zheng, Deterministic entanglement swapping in a superconducting circuit, arXiv: 1902.10959 (2019)
41. Z. Yan, Y. R. Zhang, M. Gong, Y. Wu, Y. Zheng, S. Li, C. Wang, F. Liang, J. Lin, Y. Xu, C. Guo, L. Sun, C. Z. Peng, K. Xia, H. Deng, H. Rong, J. Q. You, F. Nori, H. Fan, X. Zhu, and J. W. Pan, Strongly correlated quantum walks with a 12-qubit superconducting processor, *Science* 364(6442), 753 (2019)
42. W. Chen, D. A. Bennett, V. Patel, and J. E. Lukens, Substrate and process dependent losses in superconducting thin film resonators, *Supercond. Sci. Technol.* 21(7), 075013 (2008)
43. P. J. Leek, M. Baur, J. M. Fink, R. Bianchetti, L. Steffen, S. Filipp, and A. Wallraff, Cavity quantum electrodynamics with separate photon storage and qubit readout modes, *Phys. Rev. Lett.* 104(10), 100504 (2010)
44. M. Reagor, W. Pfaff, C. Axline, R. W. Heeres, N. Ofek, K. Sliwa, E. Holland, C. Wang, J. Blumoff, K. Chou, M. J. Hatridge, L. Frunzio, M. H. Devoret, L. Jiang, and R. J. Schoelkopf, A quantum memory with near-millisecond coherence in circuit QED, *Phys. Rev. B* 94(1), 014506 (2016)
45. M. H. Devoret and R. J. Schoelkopf, Superconducting circuits for quantum information: An outlook, *Science* 339(6124), 1169 (2013)
46. M. Mariantoni, M. J. Storz, F. K. Wilhelm, W. D. Oliver, A. Emmert, A. Marx, R. Gross, H. Christ, and E. Solano, On-chip microwave Fock states and quantum homodyne measurements, arXiv: cond-mat/0509737 (2005)
47. Y. X. Liu, L. F. Wei, and F. Nori, Generation of non-classical photon states using a superconducting qubit in a microcavity, *Europhys. Lett.* 67(6), 941 (2004)
48. K. Moon and S. M. Girvin, Theory of microwave parametric down-conversion and squeezing using circuit QED, *Phys. Rev. Lett.* 95(14), 140504 (2005)
49. F. Marquardt and C. Bruder, Superposition of two mesoscopically distinct quantum states: Coupling a Cooper-pair box to a large superconducting island, *Phys. Rev. B* 63(5), 054514 (2001)
50. Y. X. Liu, L. F. Wei, and F. Nori, Preparation of macroscopic quantum superposition states of a cavity field via coupling to a superconducting charge qubit, *Phys. Rev. A* 71(6), 063820 (2005)
51. J. Q. Liao, J. F. Huang, and L. Tian, Generation of macroscopic Schrödinger-cat states in qubit-oscillator systems, *Phys. Rev. A (Coll. Park)* 93(3), 033853 (2016)
52. X. Y. Lü, G. L. Zhu, L. L. Zheng, and Y. Wu, Entanglement and quantum superposition induced by a single photon, *Phys. Rev. A (Coll. Park)* 97(3), 033807 (2018)
53. F. W. Strauch, K. Jacobs, and R. W. Simmonds, Arbitrary control of entanglement between two superconducting resonators, *Phys. Rev. Lett.* 105(5), 050501 (2010)
54. C. P. Yang, Q. P. Su, and S. Han, Generation of Greenberger–Horne–Zeilinger entangled states of photons in multiple cavities via a superconducting qutrit or an atom through resonant interaction, *Phys. Rev. A* 86(2), 022329 (2012)
55. P. B. Li, S. Y. Gao, and F. L. Li, Engineering two-mode entangled states between two superconducting resonators by dissipation, *Phys. Rev. A* 86(1), 012318 (2012)

56. C. P. Yang, Q. P. Su, S. B. Zheng, and S. Han, Generating entanglement between microwave photons and qubits in multiple cavities coupled by a superconducting qutrit, *Phys. Rev. A* 87(2), 022320 (2013)
57. Q. P. Su, H. H. Zhu, L. Yu, Y. Zhang, S. J. Xiong, J. M. Liu, and C. P. Yang, Generating double NOON states of photons in circuit QED, *Phys. Rev. A* 95(2), 022339 (2017)
58. C. P. Yang, Q. P. Su, S. B. Zheng, F. Nori, and S. Han, Entangling two oscillators with arbitrary asymmetric initial states, *Phys. Rev. A* 95(5), 052341 (2017)
59. S. T. Merkel and F. K. Wilhelm, Generation and detection of NOON states in superconducting circuits, *New J. Phys.* 12(9), 093036 (2010)
60. Y. J. Zhao, C. Q. Wang, X. Zhu, and Y. X. Liu, Engineering entangled microwave photon states via multiphoton transitions between two cavities and a superconducting qubit, arXiv: 1506.06363 (2015)
61. S. J. Xiong, Z. Sun, J. M. Liu, T. Liu, and C. P. Yang, Efficient scheme for generation of photonic NOON states in circuit QED, *Opt. Lett.* 40(10), 2221 (2015)
62. M. Hua, M. J. Tao, and F. G. Deng, Universal quantum gates on microwave photons assisted by circuit quantum electrodynamics, *Phys. Rev. A* 90(1), 012328 (2014)
63. M. Hua, M. J. Tao, and F. G. Deng, Fast universal quantum gates on microwave photons with all-resonance operations in circuit QED, *Sci. Rep.* 5(1), 9274 (2015)
64. B. Ye, Z. F. Zheng, Y. Zhang, C. P. Yang, and Q. E. D. Circuit, single-step realization of a multiqubit controlled phase gate with one microwave photonic qubit simultaneously controlling $n - 1$ microwave photonic qubits, *Opt. Express* 26(23), 30689 (2018)
65. M. Hofheinz, H. Wang, M. Ansmann, R. C. Bialczak, E. Lucero, M. Neeley, A. D. O'Connell, D. Sank, J. Wenner, J. M. Martinis, and A. N. Cleland, Synthesizing arbitrary quantum states in a superconducting resonator, *Nature* 459(7246), 546 (2009)
66. M. Hofheinz, E. M. Weig, M. Ansmann, R. C. Bialczak, E. Lucero, M. Neeley, A. D. O'Connell, H. Wang, J. M. Martinis, and A. N. Cleland, Generation of Fock states in a superconducting quantum circuit, *Nature* 454(7202), 310 (2008)
67. H. Wang, M. Hofheinz, M. Ansmann, R. C. Bialczak, E. Lucero, M. Neeley, A. D. O'Connell, D. Sank, J. Wenner, A. N. Cleland, and J. M. Martinis, Measurement of the decay of Fock states in a superconducting quantum circuit, *Phys. Rev. Lett.* 101(24), 240401 (2008)
68. Y. Xu, W. Cai, Y. Ma, X. Mu, W. Dai, W. Wang, L. Hu, X. Li, J. Han, H. Wang, Y. Song, Z. B. Yang, S. B. Zheng, and L. Sun, Geometrically manipulating photonic Schrödinger cat states and realizing cavity phase gates, arXiv: 1810.04690 (2018)
69. H. Wang, M. Mariantoni, R. C. Bialczak, M. Lenander, E. Lucero, M. Neeley, A. D. O'Connell, D. Sank, M. Weides, J. Wenner, T. Yamamoto, Y. Yin, J. Zhao, J. M. Martinis, and A. N. Cleland, Deterministic entanglement of photons in two superconducting microwave resonators, *Phys. Rev. Lett.* 106(6), 060401 (2011)
70. M. Mariantoni, H. Wang, R. C. Bialczak, M. Lenander, E. Lucero, M. Neeley, A. D. O'Connell, D. Sank, M. Weides, J. Wenner, T. Yamamoto, Y. Yin, J. Zhao, J. M. Martinis, and A. N. Cleland, Photon shell game in three-resonator circuit quantum electrodynamics, *Nat. Phys.* 7(4), 287 (2011)
71. L. Hu, Y. Ma, W. Cai, X. Mu, Y. Xu, W. Wang, Y. Wu, H. Wang, Y. P. Song, C. L. Zou, S. M. Girvin, L. M. Duan, and L. Sun, Quantum error correction and universal gate set operation on a binomial bosonic logical qubit., *Nat. Phys.* 15(5), 503 (2019)
72. R. W. Heeres, P. Reinhold, N. Ofek, L. Frunzio, L. Jiang, M. H. Devoret, and R. J. Schoelkopf, Implementing a universal gate set on a logical qubit encoded in an oscillator, *Nat. Commun.* 8(1), 94 (2017)
73. N. Ofek, A. Petrenko, R. Heeres, P. Reinhold, Z. Leghtas, B. Vlastakis, Y. Liu, L. Frunzio, S. M. Girvin, L. Jiang, M. Mirrahimi, M. H. Devoret, and R. J. Schoelkopf, Extending the lifetime of a quantum bit with error correction in superconducting circuits, *Nature* 536(7617), 441 (2016)
74. C. P. Yang and Z. F. Zheng, Deterministic generation of Greenberger-Horne-Zeilinger entangled states of cat-state qubits in circuit QED, *Opt. Lett.* 43(20), 5126 (2018)
75. M. Mirrahimi, Z. Leghtas, V. V. Albert, S. Touzard, R. J. Schoelkopf, L. Jiang, and M. H. Devoret, Dynamically protected cat-qubits: A new paradigm for universal quantum computation, *New J. Phys.* 16(4), 045014 (2014)
76. S. E. Nigg, Deterministic Hadamard gate for microwave cat-state qubits in circuit QED, *Phys. Rev. A* 89(2), 022340 (2014)
77. Y. Zhang, X. Zhao, Z. F. Zheng, L. Yu, Q. P. Su, and C. P. Yang, Universal controlled-phase gate with cat-state qubits in circuit QED, *Phys. Rev. A* 96(5), 052317 (2017)
78. Y. J. Fan, Z. F. Zheng, Y. Zhang, D. M. Lu, and C. P. Yang, One-step implementation of a multi-target-qubit controlled phase gate with cat-state qubits in circuit QED, *Front. Phys.* 14(2), 21602 (2019)
79. R. W. Heeres, P. Reinhold, N. Ofek, L. Frunzio, L. Jiang, M. H. Devoret, and R. J. Schoelkopf, Implementing a universal gate set on a logical qubit encoded in an oscillator, *Nat. Commun.* 8(1), 94 (2017)
80. C. Wang, Y. Y. Gao, P. Reinhold, R. W. Heeres, N. Ofek, K. Chou, C. Axline, M. Reagor, J. Blumoff, K. M. Sliwa, L. Frunzio, S. M. Girvin, L. Jiang, M. Mirrahimi, M. H. Devoret, and R. J. Schoelkopf, A Schrodinger cat living in two boxes, *Science* 352(6289), 1087 (2016)
81. P. J. Leek, S. Filipp, P. Maurer, M. Baur, R. Bianchetti, J. M. Fink, M. Göppl, L. Steffen, and A. Wallraff, Using sideband transitions for two-qubit operations in superconducting circuits, *Phys. Rev. B* 79(18), 180511 (2009)
82. M. Sandberg, C. M. Wilson, F. Persson, T. Bauch, G. Johansson, V. Shumeiko, T. Duty, and P. Delsing, Tuning the field in a microwave resonator faster than the photon lifetime, *Appl. Phys. Lett.* 92(20), 203501 (2008)
83. D. F. V. James and J. Jerke, Effective Hamiltonian theory and its applications in quantum information, *Can. J. Phys.* 85(6), 625 (2007)

84. J. Q. You, X. Hu, S. Ashhab, and F. Nori, Low-decoherence flux qubit, *Phys. Rev. B* 75, 140515(R) (2007)
85. M. Steffen, S. Kumar, D. P. DiVincenzo, J. R. Rozen, G. A. Keefe, M. B. Rothwell, and M. B. Ketchen, High-coherence hybrid superconducting qubit, *Phys. Rev. Lett.* 105(10), 100502 (2010)
86. F. Yan, S. Gustavsson, A. Kamal, J. Birenbaum, A. P. Sears, D. Hover, T. J. Gudmundsen, D. Rosenberg, G. Samach, S. Weber, J. L. Yoder, T. P. Orlando, J. Clarke, A. J. Kerman, and W. D. Oliver, The flux qubit revisited to enhance coherence and reproducibility, *Nat. Commun.* 7(1), 12964 (2016)
87. M. Baur, S. Filipp, R. Bianchetti, J. M. Fink, M. Göppl, L. Steffen, P. J. Leek, A. Blais, and A. Wallraff, Measurement of Autler-Townes and Mollow transitions in a strongly driven superconducting qubit, *Phys. Rev. Lett.* 102(24), 243602 (2009)
88. F. Yoshihara, Y. Nakamura, F. Yan, S. Gustavsson, J. Bylander, W. D. Oliver, and J. S. Tsai, Flux qubit noise spectroscopy using Rabi oscillations under strong driving conditions, *Phys. Rev. B* 89(2), 020503 (2014)